

Sliding stability analysis of a retaining wall constructed by soilbags

K. FAN*†, S. H. LIU*, Y. P. CHENG† and Y. WANG*

Model tests were conducted to analyse the sliding stability of a retaining wall constructed by soilbags. The aim was to obtain an equation that calculates the active resultant earth pressure of sand acting on the wall in the ultimate state. Additionally, shear tests on multi-layers of vertically stacked soilbags were designed to investigate how the interlayer friction resistance varied with the height of the wall. The results show that the active earth pressure acting on the soilbag-constructed retaining wall in the ultimate state is non-linear, but it can be calculated from the force equilibrium of a differential element. The interlayer friction resistance of soilbags is found to be related to the shape of the sliding surface. Based on the obtained equation and the unique shear test results, the sliding stability of the retaining wall constructed by soilbags could be appropriately analysed.

KEYWORDS: earth pressure; retaining walls; sands

ICE Publishing: all rights reserved

NOTATION

| | |
|------------|--|
| d_y | thickness of the differential flat element |
| dW | weight of the differential element |
| H_{crit} | height of the wall above the slip surface |
| K | active lateral pressure coefficient |
| p_x | horizontal reaction on the wall |
| p_y | vertical reaction on the wall |
| q | uniformly distributed stress on wall's top surface |
| r | normal reaction of the soil at rest |
| y | depth from the surface of the backfill |
| γ | unit weight of the backfill |
| δ | frictional angle between the back of the wall and the backfill |
| θ | horizontal angle of the failure line $\theta = \arctan(\tan \phi + \sqrt{\tan^2 \phi + \tan \phi / \tan(\phi + \delta)})$ |
| τ_1 | shear between the backfill and the back of the retaining wall |
| τ_2 | shear between the sliding backfill and the remaining backfill at rest |
| ϕ | internal friction angle of the backfill |

INTRODUCTION

Soilbags or more exactly geotextile bags filled with soil or soil-like materials which are commonly used to build embankments during floods, and to construct temporary structures after disasters (Kim *et al.*, 2004). Early research was concentrated in investigating the mechanical behaviour of individual soilbags. Matsuoka & Liu (2003) found that soilbags have a very high compressive strength from experimental and theoretical studies. The high compressive strength of soilbags can be theoretically explained by the increased apparent cohesion that develops due to the tensile force of the wrapped bag under external loading; this theory was further verified by numerous researchers (Tantonio & Bauer, 2008; Xu *et al.*, 2008; Cheng *et al.*, 2016; Liu *et al.*, 2018). Ansari *et al.* (2011) numerically analysed the mechanical behaviour of a soilbag subject to compression and lateral cyclic shear loading; they reported that

the stiffness and the compressive load capacity of a soilbag are considerably higher than those of an unwrapped granular material. Since then, soilbags have been widely used to reinforce foundations (Liu *et al.*, 2014; Ding *et al.*, 2017, 2018) and to construct retaining walls (Portelinha *et al.*, 2014; Wang *et al.*, 2015; Liu *et al.*, 2019), slopes (Huang *et al.*, 2008; Liu *et al.*, 2012, 2015; Wen *et al.*, 2016) and small dams (Li *et al.*, 2017). Soilbags can be filled at the site using the in situ soil (e.g. a 5 m high wall reported by Liu *et al.*, 2019) or prepared remotely in advance and transported to the site (e.g. more than a 20 m high slope of the south-to-north water transfer project in China reported by Liu *et al.*, 2015).

Retaining walls constructed by soilbags generally have the advantages of low cost, light weight, good adaptation to foundation deformation and good seismic performance similar to geosynthetically reinforced earth retaining wall (Matsuoka & Liu, 2014). Currently, the soils that have been used as filling material in soilbags include natural river sand (Matsushima *et al.*, 2008; Liu *et al.*, 2016), clayey soils (Liu *et al.*, 2019), small-size stones, expansive soil (Liu *et al.*, 2015; Wang *et al.*, 2015), loam soils (Liu *et al.*, 2016) dry ash (Li *et al.*, 2017) and so on. The common features of these soils are that the particle sizes are relatively small such that they can be filled into the bags easily, and do not have obvious sharp edges or corners so they cannot easily cut through the bags. These fill materials for soilbags were found to not significantly affect the overall performance (Matsuoka & Liu, 2014). Due to these advantages, soilbags have been widely used in many projects with retaining walls (Liu, 2017). However, when compared with concrete gravity retaining walls, the retaining walls constructed by soilbags are thicker. Moreover, protective measures such as thick concrete facing or masonry facing should be considered to prevent bags from being directly exposed to ultraviolet radiation. Additionally, there is still no appropriately documented design guideline. Matsushima *et al.* (2008) showcased many examples of soilbag-constructed retaining walls failure, and found that one of the major drawbacks of this type of wall is the relatively low stability caused by slippage along the horizontal interface in between the adjacent soilbags, which results in a catastrophic failure. Hence, sliding stability should be the most important issue in the design of a retaining wall constructed with soilbags. It was also stated (Matsushima *et al.*, 2008) that the shear strength of

Manuscript received 5 January 2019; first decision 3 May 2019; accepted 21 May 2019.

*College of Water Conservancy and Hydropower, Hohai University, Nanjing, China.

†Civil, Environmental and Geomatic Engineering, University College London, London, UK.

multi-layered soilbags is highly anisotropic when they are stacked horizontally and inclined, but only the sliding stability of the retaining wall constructed with horizontally stacked soilbags, usually used in practical engineering, is studied in this paper.

To analyse the sliding stability of these walls, this paper presents model tests of soilbag-constructed retaining wall and simple shear tests on five layers of vertically stacked soilbags. In the model test, the displacement, sliding surface and lateral earth pressure of the wall were monitored. An equation for calculating the active earth pressure on the retaining wall of soilbags in the ultimate state was derived from the force equilibrium of a differential element. The interlayer friction resistance of soilbags was then obtained from the shear tests to analyse the sliding stability.

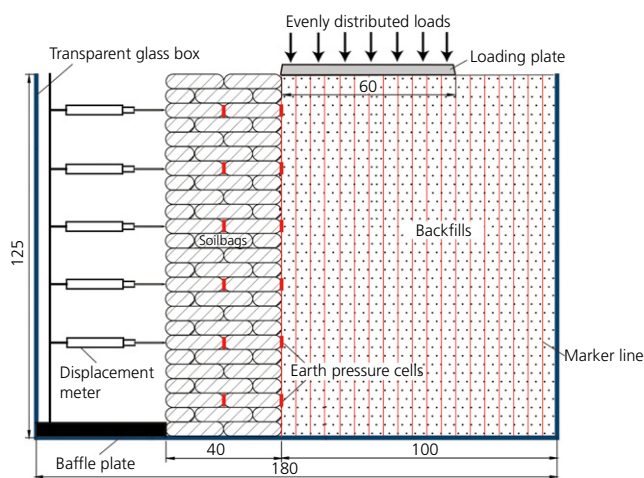
ACTIVE EARTH PRESSURE AT FAILURE

Model test

The model tests were performed in a cuboid box 180 cm long, 80 cm wide and 140 cm high, as shown in Fig. 1. Two sheets of 2 cm thick glass, which were rigid enough against deformation, were placed on the inner faces of the box to reduce side friction and for observation. A soilbag-constructed wall with a height of 125 cm was set up in the box. Soilbags of two sizes (20 cm × 20 cm × 5 cm and



(a)



(b)

Fig. 1. Photograph and schematic view of the model test (unit: cm): (a) photo, (b) schematic diagram

Table 1. Physical and mechanical parameters of natural river sand

| D_{30} : mm | D_{50} : mm | D_{60} : mm | D_{90} : mm | C_u | C_c | ϕ : deg |
|---------------|---------------|---------------|---------------|-------|-------|--------------|
| 0.32 | 0.36 | 0.4 | 0.75 | 2 | 1.28 | 35.4 |

20 cm × 10 cm × 5 cm) were staggered as shown in Fig. 1 to construct the model wall. Behind the wall dry river sand (see Table 1 for its physical and mechanical properties) was placed in layers and compacted by tamping to a desired relative density of 70% ($\rho = 1.76 \text{ g/cm}^3$) using a hand-operated vibrator. On the top surface of the backfill, vertical uniform loads were applied to a loading plate with a size of 70 cm × 60 cm using an oil jack. The width of the loading plate is smaller than that of the sand box as it is easier to put the loading plate into the box, and it prevents friction between the loading plate and the box. The applied vertical load was increased until a sliding surface appeared in the wall.

To evaluate the behaviour of the model testing the retaining wall, a number of monitoring instruments were installed as shown in Fig. 1. Twelve earth pressure cells were buried during the construction of the wall to measure the lateral earth pressures on the backfill soil and in the soilbags. Five flexible displacement meters were installed to measure the displacement of the wall face. A number of marker lines were drawn on both the inside and outside of the glass. The inside lines moved with the movement of the backfill, while the outside lines remained stationary. The displacement of the backfills could be obtained by measuring the relative displacement of the corresponding marker lines both inside and outside. A camera was positioned in front of the model test to monitor the movement of the markers at regular intervals.

The soilbags used in the model tests were filled with natural river sand (see Table 1) as backfill. The woven bags were made of polypropylene with a weight of 150 g/m². The tensile strength of the bags are 37.1 and 28.0 kN/m in warp and weft directions, respectively. The warp and weft elongations are both less than 25% at failure and the friction coefficient of the bags is 0.54.

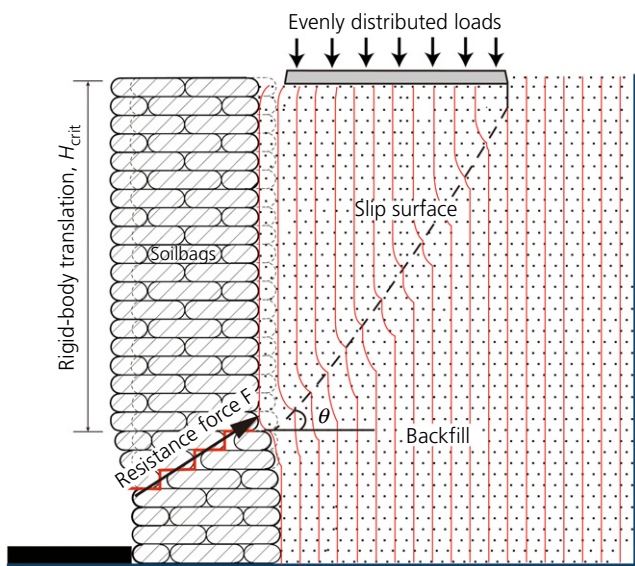
Test results

In this model test, the retaining wall failed when the vertical load applied on the loading plate reached 8.7 kPa, and a slip surface appeared in the backfill soil. The angle between the slip surface and the horizontal line is about 60°, which is close to the value of the Coulomb sliding friction angle ($\theta = 59^\circ$). As shown in Fig. 2, a ladder-like sliding surface appeared in the soilbag-constructed retaining wall, which runs through three layers of soilbags. The top of the ladder-like surface appeared to be connected to the bottom of the slip surface. The wall above the ladder-like surface undergoes a rigid-body translation, and the height H_{crit} of it is 0.95 m.

Figure 3 shows the stacked soilbags which are arranged in a staggered manner. Due to the flexibility of soilbags, the soilbag in the upper layer can deform into the gaps between soilbags in the lower layer, with embedded contacts when subjected to vertical load; this is defined as the interlayer insertion in this paper. The authors believe that the formation of this ladder-like sliding surface is the result of the interlayer insertion of soilbags. Figure 4 shows the experimental distribution of earth pressure (measured) under ultimate load. It can be seen that the earth pressure



(a)



(b)

Fig. 2. Deformation of the retaining wall and backfills: (a) photo, (b) schematic diagram

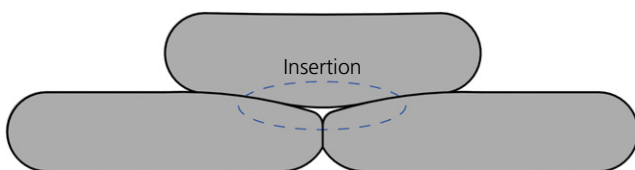


Fig. 3. Schematic view of the insertion between two layers of soilbags

acting on the wall is non-linear, which is different from the linear prediction under the assumption of Coulomb's theory.

Active resultant earth pressure calculation

A correct estimation of the magnitude and distribution of the active earth pressure acting on the retaining structures is important for safety, economical design and construction. Coulomb's theory assumes a linear distribution of the active earth pressure and has been widely used for that purpose.

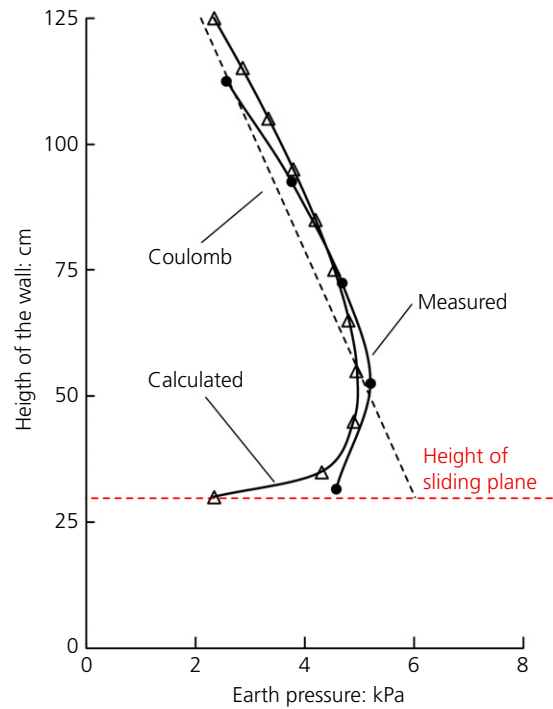


Fig. 4. Distribution of the lateral earth pressures on backfills and within the soilbags under ultimate load

However, many experimental and field data (Tsagareli, 1965; Sherif *et al.*, 1984; O'Neal & Hagerty, 2011; Khosravi *et al.*, 2013; Vo *et al.*, 2016) showed that the distribution of the active earth pressure behind a wall is non-linear, indicating that the Coulomb's theory is not appropriate. Many investigations have been conducted to study the non-linear active earth pressures associating the mode of wall movement with the force equilibrium of a differential element, and preferable results have been achieved (Wang, 2000; Paik & Salgado, 2003; Goel & Patra, 2008). Following this approach in this model test, the non-linear active earth pressures acting on the soilbag-constructed retaining wall is calculated by a differential element method.

On the basis of the model test results, it is first assumed that the earth pressure against the back of the wall is due to the thrust exerted by the sliding wedge when the wall moves forward. Taking the sliding wedge as an isolated unit, as shown in Fig. 5(a), a differential flat element of thickness, dy is taken from the wedge at a depth, y below the ground surface. From Fig. 5(b), the forces acting on this element include the vertical pressure, p_y on the top of the element, the vertical reaction, $p_y + dp_y$ on the bottom of the element, the horizontal reaction, p_x of the retaining wall, the shear, τ_1 between the backfill and the back of the retaining wall, the normal reaction, r of the soil at rest, the shear, τ_2 between the sliding backfill and the remaining backfill at rest and the weight, dW of the element.

By analysing the stress of the differential element, Wang (2000) derived the following expression of the horizontal unit earth pressure

$$p_x = K \left[\left(q - \frac{\gamma H_{crit}}{\alpha K - 2} \right) \left(\frac{H_{crit} - y}{H_{crit}} \right)^{\alpha K - 1} + \frac{\gamma}{\alpha K - 2} H_{crit} - y \right] \tag{1}$$

where q is the uniformly distributed stress on wall's top surface and q is obtained by dividing the force loaded in the loading plate by the corresponding area of the backfill (80 cm × 60 cm). K is the active lateral pressure coefficient,

$K = p_x/p_y$. $\alpha = (\cos(\theta - \phi - \delta)/\sin(\theta - \phi)) (\tan \theta/\cos \delta)$, in which ϕ is the internal friction angle of the backfill, and δ is the frictional angle between the back of the wall and the backfill. The detailed derivation is shown in the Appendix.

The resultant earth pressure is given by

$$P_x = \int_0^h p_x dy = KqH_{crit} + \frac{1}{2\alpha} \gamma H_{crit}^2 \quad (2)$$

However, Wang (2000) did not give an expression for the active lateral pressure coefficient. Paik and Salgado (2003)

proposed an equation to calculate the active lateral pressure coefficient under the assumptions that the trajectory of the minor principal stress takes the shape of a circular arc, giving

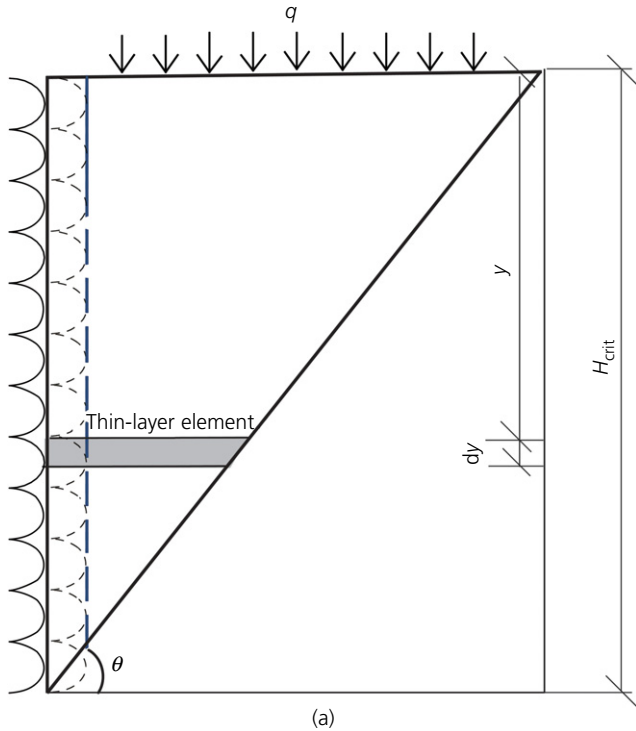
$$K = \frac{3(m \cos^2 \omega + \sin^2 \omega)}{3m - (m - 1) \cos^2 \omega} \quad (3)$$

in which

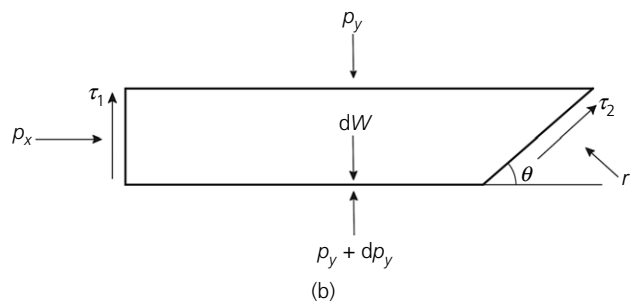
$$\omega = \arctan \left[\frac{m - 1 + \sqrt{(m - 1)^2 - 4m \tan \delta}}{2 \tan \delta} \right],$$

$$m = \tan^2(45^\circ + \phi/2)$$

In the model test, natural river sand was used as the backfill, with a unit weight $\gamma = 17.6 \text{ kN/m}^3$ and internal friction angle $\phi = 35.4^\circ$. Separate shear tests were conducted by vertically loading a single soilbag that was placed on a large box filled with sand to obtain the relationship between the shear force acting on the soilbag and the applied normal stress. This was used to calculate the frictional angle between the back of the wall and the backfill ($\delta = 28.1^\circ$). The earth's pressure calculated using the equations presented above is shown in Fig. 4, and it can be seen that this provides a better agreement with the experiment data than that obtained by Coulomb's theory.



(a)



(b)

Fig. 5. Analytic model: (a) deformation mode of the backfill soil behind the retaining wall of soilbags, (b) analysis of the forces acting on the thin-layer element

INTERLAYER FRICTION

Liu *et al.* (2016) found that the interlayer friction of soilbags is the major factor for maintaining the sliding stability of a retaining wall constructed with soilbags. Here, a special simple-shear apparatus as shown in Fig. 6 was designed to obtain the correct interlayer friction of the soilbags with the increasing height of the wall. As the interlayer friction of the soilbags acted along a ladder-like failure surface in the retaining wall, simple direct shear tests using only two layers of vertically stacked soilbags were inappropriate. Instead, simple shear tests using five layers of vertically stacked soilbags were carried out. The different vertical loads, N imposed by the iron plates correspond to different additional heights of the soilbag-constructed retaining wall. The measured shear force corresponds to the interlayer sliding force, F . In fact, as the lateral earth pressure on the retaining wall constructed with soilbags generates moment that increases with an increase of the wall height, the distribution of the applied vertical pressure on the soilbags is not uniform but eccentric. However, due to the limitations of the test equipment, the moment generated by the application of the lateral load was not applied in the tests.

Figure 7 shows the relationship between shear force and shear displacement measured during the simple shear tests. It can be seen that the shear force increased with an increase

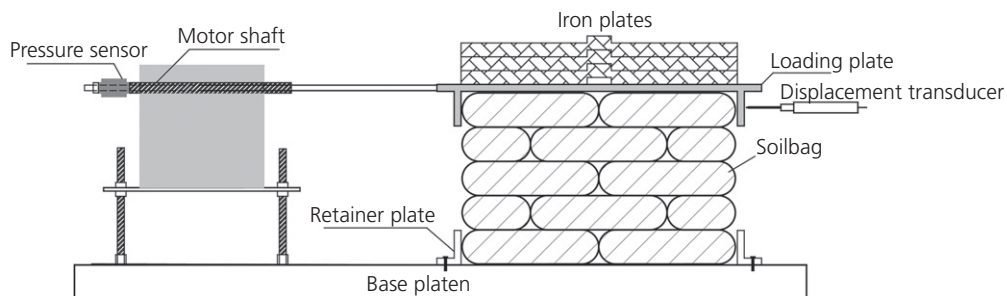


Fig. 6. Schematic view of the simple shear test on stacked soilbags

in the lateral shear displacement under different vertical loads, and the peak shear strength increased with an increase of the vertical loads. Shear tests on two layers of vertically

stacked soilbags (Fig. 8) were also performed; the peak shear strength result is given in Fig. 7(b). As shown in the figure, the peak shear strength of the five layers of vertically stacked soilbags is larger than that of the two vertically stacked soilbags. As we know, the friction F can be expressed as

$$F = \mu N$$

where μ is the friction coefficient and N is the vertical load.

As the same soilbags as those used in the shear tests on five layers of soilbags and were used in that of the two-layer soilbag tests, μ should be the same. However, Fig. 8(b) shows that there is a difference between the two curves: curve A is a straight line, but curve B is not, and the difference is explained in Figure 9. The sliding surface in the shear tests using two layers of soilbags is purely the interface between the soilbags, but the sliding surface in the tests using five layers of soilbags is not. When H_{crit} is no more than 5 cm, the sliding surface of the five-layer test is almost horizontal, as shown in Fig. 9(a), while the sliding surface is ladder like, as shown in Fig. 9(b), when H_{crit} is larger than 25 cm. This is the same ladder-like sliding surface as seen previously in the model test (Fig. 2). The reason why the shape of the sliding surface changes from being a straight line to ladder like is that the insertion of soilbags increases with the vertical load. Hence, the horizontal force applied at the upper layer soilbags was partially distributed to the soilbags at a lower layer. A more in-depth study of this mechanism will be explored in a separate paper.

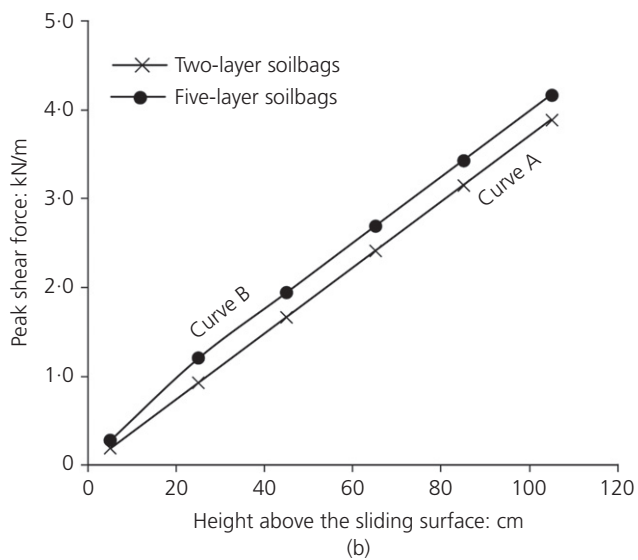
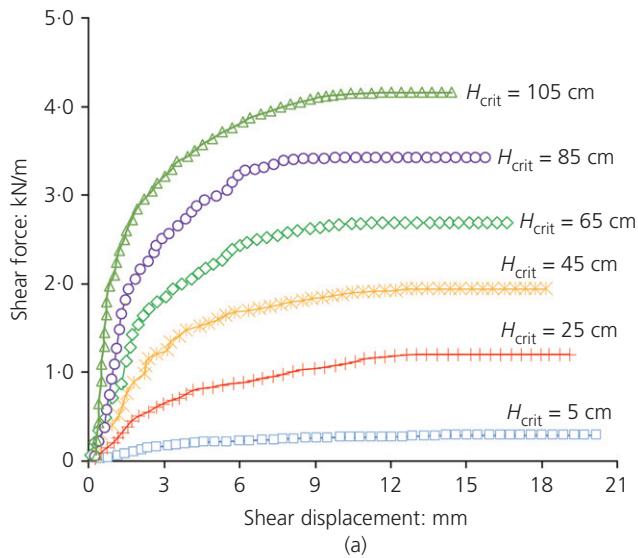


Fig. 7. Results of the simple shear tests on vertically stacked soilbags: (a) shear force F against horizontal shear displacement, (b) peak shear force F_p against the critical wall height H_{crit} above the sliding surface

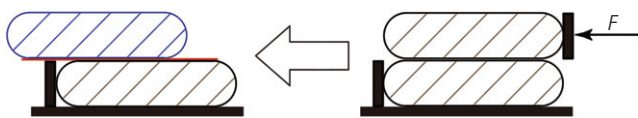


Fig. 8. Slip surface in the shear tests on two-layer soilbags

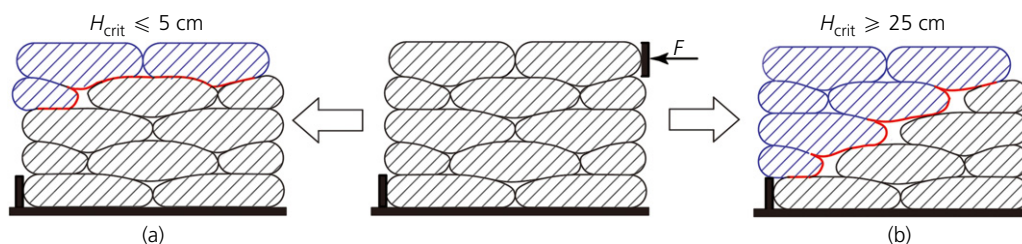


Fig. 9. Different sliding surfaces in the shear tests on five-layer soilbags: (a) I sliding surface, (b) II sliding surface

SLIDING STABILITY ANALYSIS

After obtaining the active resultant earth pressure and the interlayer friction resistance, the sliding stability of the retaining wall constructed with soilbags can be analysed. Figure 10 shows the resultant earth pressure calculated using equation (2) and the interlayer friction resistance (Fig. 7). When $F(h) = P(h)$, it is found that H_{crit} is 0.915 m, whereas the experimental result is 0.95 m, and the difference is smaller than the height of one soilbag (0.05 m). However, H_{crit} would be 1.04 m if using the resultant earth pressure calculated by Coulomb's theory. The overestimation is 0.09 m, which is approximately two layers of soilbags. It should be noted that regardless of it being simple and easy to operate, there is a limitation in this study: With the use of a loading plate to exert a vertical load on the backfills, the retaining wall fails cannot completely restore the general loading condition, but they may produce a slightly different ratio between the lateral and vertical load compared to the actual retaining walls.

CONCLUSIONS

Model tests on soilbag-constructed retaining walls and simple-shear tests on vertically stacked soilbags were carried out to analyse the sliding stability of the wall.

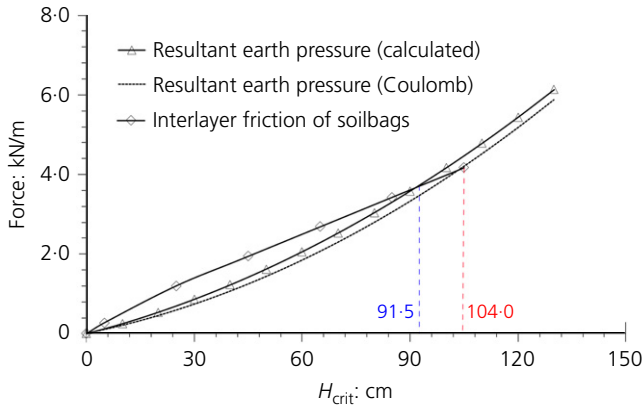


Fig. 10. Resultant earth pressure and interlayer friction of soilbags with the height of the retaining wall

Based on the test results, the following conclusions were made.

- The sliding surface developed within the wall of the soilbags is not a straight line, but ladder like due to the insertion characteristic of the soilbags. The wall above the ladder-like sliding surface was found to undergo a rigid-body translation.
- Horizontal sliding failure of the wall creates a non-linear active earth pressure distribution at failure. Calculations using force equilibrium of differential elements produces a better match to the experimental data than Coulomb's theory.
- The sliding friction resistance of the wall is found to be related to the shape of the interlayer sliding surface of the soilbags. When the wall height is small, the sliding surface is horizontal; when the wall height is large, the sliding surface is ladder like. This result was obtained from a specially designed shear apparatus for stacked soilbags. The chosen number of soilbags used in the shear tests depends on both the actual thickness of the wall and the potential height of the sliding surface.
- The sliding stability of the retaining wall constructed with soilbags could be appropriately obtained using the intersection of failure of earth pressure calculated by differential elements and the sliding friction resistance obtained from the shear tests. This proposed method can be adopted for the design of a soilbag-constructed retaining wall.

ACKNOWLEDGEMENTS

This work was supported by the National Key R&D Program of China (grant number 2017YFC0404805) and the China Scholarship Council (number 201806710071).

APPENDIX

It can be shown (Fig. 5) from the equilibrium condition of the horizontal forces on the element, that

$$p_x dy + \tau_2 \frac{dy}{\sin \theta} \cos \theta - r \times \frac{dy}{\sin \theta} \cos(90^\circ - \theta) = 0 \quad (4)$$

Equation (4) can be written as

$$p_x + \tau_2 \cot \theta - r = 0 \quad (5)$$

The following equation can be obtained from the equilibrium condition of the vertical forces on the element

$$p_y (H_{\text{crit}} - y) \cot \theta + dW - (p_y + dp_y)(H_{\text{crit}} - y - dy) \times \cot \theta - \tau_1 dy - \tau_2 \frac{dy}{\sin \theta} \sin \theta - r \times \frac{dy}{\cos \theta} \sin \theta = 0 \quad (6)$$

where $dW = ((H_{\text{crit}} - y) \cot \theta + (H_{\text{crit}} - y - dy) \cot \theta) dy/2 \gamma$

Substitute dW into equation (6), and omit the second-order differential terms, equation (6) can be simplified to

$$\frac{dp_y}{dy} = \gamma + \frac{1}{H_{\text{crit}} - y} [p_y - r - (\tau_1 + \tau_2) \tan \theta] \quad (7)$$

Let

$$\begin{aligned} p_x &= K p_y \\ \tau_1 &= p_x \tan \delta \\ \tau_2 &= r \tan \phi \end{aligned} \quad (8)$$

where K is the active lateral pressure coefficient at failure, δ is the frictional angle between the back of the wall and the backfill and ϕ is the internal friction angle of the backfill.

Substituting equation (8) into equation (5), it can be shown that

$$r = K \frac{\sin \theta \cos \phi}{\sin(\theta - \phi)} p_y \quad (9)$$

Substituting equations (8) and (9) into equation (7), the following equation can be obtained

$$\frac{dp_y}{dy} = \left[1 - \frac{\cos(\theta - \phi - \delta) \tan \theta}{\sin(\theta - \phi) \cos \delta} K \right] \frac{p_y}{H_{\text{crit}} - y} + \gamma \quad (10)$$

Let

$$\alpha = \frac{\cos(\theta - \phi - \delta) \tan \theta}{\sin(\theta - \phi) \cos \delta} \quad (11)$$

Equation (10) can be written as

$$\frac{dp_y}{dy} = -(aK - 1) \frac{p_y}{H_{\text{crit}} - y} + \gamma \quad (12)$$

By differentiation, the general solution of equation (12) is

$$p_y = A \frac{1}{K} (H_{\text{crit}} - y)^{aK-1} + \frac{\gamma}{aK-2} (H_{\text{crit}} - y) \quad (13)$$

in which A is a constant, which can be determined by the boundary condition. Suppose that a surcharge q is exerted on the backfill surface – that is, $p_y = q$ when $y=0$. Substituting equation (13) into the boundary condition, the constant A can be determined as

$$A = \left(q - \frac{\gamma H_{\text{crit}}}{aK-2} \right) \frac{K}{H_{\text{crit}}^{aK-1}} \quad (14)$$

Substituting equation (14) into equation (13), this leads to

$$p_y = \left(q - \frac{\gamma H_{\text{crit}}}{aK-2} \right) \left(\frac{H_{\text{crit}} - y}{H_{\text{crit}}} \right)^{aK-1} + \frac{\gamma}{aK-2} H_{\text{crit}} - y \quad (15)$$

According to equation (8), $p_x = K p_y$, so that the horizontal unit earth pressure can be obtained

$$p_x = K \left[\left(q - \frac{\gamma H_{\text{crit}}}{aK-2} \right) \left(\frac{H_{\text{crit}} - y}{H_{\text{crit}}} \right)^{aK-1} + \frac{\gamma}{aK-2} H_{\text{crit}} - y \right] \quad (16)$$

REFERENCES

- Ansari, Y., Merifield, R., Yamamoto, H. & Sheng, D. (2011). Numerical analysis of soilbags under compression and cyclic shear. *Geotex. Geomembr.* **38**, No. 5, 659–668.
- Cheng, H., Yamamoto, H. & Thoeni, K. (2016). Numerical study on stress states and fabric anisotropies in soilbags using the DEM. *Comput. Geotech.* **76**, 170–183.
- Ding, G., Wu, J., Wang, J. & Hu, X. (2017). Effect of sand bags on vibration reduction in road subgrade. *Soil Dyn. Earthq. Engng* **100**, 529–537.
- Ding, G., Wu, J., Wang, J., Fu, H. & Liu, F. J. G. I. (2018). Experimental study on vibration reduction by using soilbag cushions under traffic loads. *Geosyn. Int.* **25**, No. 3, 322–333.
- Goel, S. & Patra, N. (2008). Effect of arching on active earth pressure for rigid retaining walls considering translation mode. *Int. J. Geomech.* **8**, No. 2, 123–133.
- Huang, C. C., Matsushima, K., Mohri, Y. & Tatsuoka, F. (2008). Analysis of sand slopes stabilized with facing of soil bags with extended reinforcement strips. *Geosyn. Int.* **15**, No. 4, 232–245, <https://doi.org/10.1680/gein.2008.15.4.232>.
- Khosravi, M., Pipatpongsa, T. & Takemura, J. (2013). Experimental analysis of earth pressure against rigid retaining walls under translation mode. *Géotechnique* **63**, No. 12, 1020–1028, <https://doi.org/10.1680/geot.12.P021>.
- Kim, M., Freeman, M., Fitzpatrick, B. T., Nevius, D. B., Plaut, R. H. & Filz, G. M. (2004). Use of an apron to stabilize geomembrane tubes for fighting floods. *Geotex. Geomembr.* **22**, No. 4, 239–254.
- Li, H., Song, Y., Gao, J., Li, L., Zhou, Y. & Qi, H. (2017). Construction of a dry ash dam with soilbags and slope stability analysis. In *IOP Conference series: materials science and engineering* (ed. M. Aleksandrova), vol. 275, No. 1, p. 012034. Bristol, UK: IOP Publishing.
- Liu, S. H. (2017). *Principle and application of soilbags*. Nanjing, China: Science Press (in Chinese).
- Liu, S. H., Bai, F., Wang, Y., Wang, S. & Li, Z. (2012). Treatment for expansive soil channel slope with soilbags. *J. Aerosp. Engng* **26**, No. 4, 657–666.
- Liu, S. H., Gao, J. J., Wang, Y. Q. & Weng, L. P. (2014). Experimental study on vibration reduction by using soilbags. *Geotex. Geomembr.* **42**, No. 1, 52–62.
- Liu, S. H., Lu, Y., Weng, L. & Bai, F. (2015). Field study of treatment for expansive soil/rock channel slope with soilbags. *Geotex. Geomembr.* **43**, No. 4, 283–292.
- Liu, S. H., Fan, K., Chen, X., Jia, F., Mao, H. & Lin, Y. (2016). Experimental studies on interface friction characteristics of soilbags. *Chinese J. Geotech. Engng* **38**, No. 10, 1874–1880 (in Chinese).
- Liu, S. H., Jia, F., Shen, C. M. & Weng, L. P. (2018). Strength characteristics of soilbags under inclined loads. *Geotex. Geomembr.* **46**, No. 1, 1–10.
- Liu, S. H., Fan, K. & Xu, S. (2019). Field study of a retaining wall constructed with clay-filled soilbags. *Geotex. Geomembr.* **47**, No. 1, 87–94.
- Matsuoka, H. & Liu, S. H. (2003). New earth reinforcement method by soilbags ('Donow'). *Soils Found.* **43**, No. 6, 173–188.
- Matsuoka, H. & Liu, S. H. (2014). *A new earth reinforcement method using soilbags*. London, UK: CRC Press.
- Matsushima, K., Aqil, U., Mohri, Y. & Tatsuoka, F. J. G. I. (2008). Shear strength and deformation characteristics of geosynthetic soil bags stacked horizontal and inclined. *Geosyn. Int.* **15**, No. 2, 119–135.
- O'neal, T. S. & Hagerty, D. (2011). Earth pressures in confined cohesionless backfill against tall rigid walls – a case history. *Can. Geotech. J.* **48**, No. 8, 1188–1197.
- Paik, K. & Salgado, R. (2003). Estimation of active earth pressure against rigid retaining walls considering arching effects. *Géotechnique* **53**, No. 7, 643–654, <https://doi.org/10.1680/geot.2003.53.7.643>.
- Portelinha, F., Zornberg, J. & Pimentel, V. (2014). Field performance of retaining walls reinforced with woven and nonwoven geotextiles. *Geosyn. Int.* **21**, No. 4, 270–284, <https://doi.org/10.1680/gein.14.00014>.
- Sherif, M. A., Fang, Y. S. & Sherif, R. I. (1984). Ka and Ko Behind rotating and non-yielding walls. *J. Geotech. Engng* **110**, No. 1, 41–56.
- Tantono, S. F. & Bauer, E. (2008). Numerical simulation of a soilbag under vertical compression. In *proceeding of the 12th international conference of international association for computer methods and advance in geomechanics* (ed. M. N. Jadhav), pp. 433–439. Red Hook, NY, USA: Curran.
- Tsagareli, Z. (1965). Experimental investigation of the pressure of a loose medium on retaining walls with a vertical back face and horizontal backfill surface. *Soil Mech. Found. Engng* **2**, No. 4, 197–200.
- Vo, T., Taiebat, H. & Russell, A. (2016). Interaction of a rotating rigid retaining wall with an unsaturated soil in experiments. *Géotechnique* **66**, No. 5, 366–377, <https://doi.org/10.1680/jgeot.14.P187>.
- Wang, Y. Z. (2000). Distribution of earth pressure on a retaining wall. *Géotechnique* **50**, No. 1, 83–88, <https://doi.org/10.1680/geot.2000.50.1.83>.
- Wang, L. J., Liu, S. H. & Zhou, B. (2015). Experimental study on the inclusion of soilbags in retaining walls constructed in expansive soils. *Geotex. Geomembr.* **43**, No. 1, 89–96.
- Wen, H., Wu, J. J., Zou, J. L., Luo, X., Zhang, M. & Gu, C. (2016). Model tests on the retaining walls constructed from geobags filled with construction waste. *Adv. Mater. Sci. Engng*, <http://dx.doi.org/10.1155/2016/4971312>.
- Xu, Y., Huang, J., Du, Y. & Sun, D. A. (2008). Earth reinforcement using soilbags. *Geotex. Geomembr.* **26**, No. 3, 279–289.

HOW CAN YOU CONTRIBUTE?

To discuss this paper, please submit up to 500 words to the editor at journals@ice.org.uk. Your contribution will be forwarded to the author(s) for a reply and, if considered appropriate by the editorial board, it will be published as a discussion in a future issue of the journal.